

**Effect of particle size on energy dissipation in viscoelastic granular collisions**

Dmytro Antypov and James A. Elliott\*

*Pfizer Institute for Pharmaceutical Materials Science, Department of Materials Science and Metallurgy, Pembroke Street, Cambridge, CB2 3QZ, United Kingdom*

Bruno C. Hancock

*Pfizer Global Research and Development, Groton, Connecticut 06340, USA*

(Received 16 July 2010; revised manuscript received 13 June 2011; published 8 August 2011)

We analyze the scaling properties of the Hertz-Kuwabara-Kono (HKK) model, which is commonly used in numerical simulations to describe the collision of macroscopic noncohesive viscoelastic spherical particles. Parameters describing the elastic and viscous properties of the material, its density, and the size of the colliding particles affect the restitution coefficient  $\varepsilon$  and collision time  $\tau$  only via appropriate rescaling but do not change the shape of  $\varepsilon(v)$  and  $\tau(v)$  curves, where  $v$  is the impact velocity. We have measured the restitution coefficient experimentally for relatively large (1 cm) particles of microcrystalline cellulose to deduce material parameters and then to predict collision properties for smaller microcrystalline cellulose (MCC) particles by assuming the scaling properties of the HKK model. In particular, we demonstrate that the HKK model predicts the restitution coefficient of microscopic particles of about 100  $\mu\text{m}$  to be considerably smaller than that of the macroscopic particles. In fact, the energy dissipation is so large that only completely inelastic collisions occur for weakly attractive particles. We propose a straightforward self-consistent extension to the Johnson-Kendall-Roberts (JKR) model to include dissipative forces and discuss the implications of our findings for the behavior of experimental powder systems.

DOI: [10.1103/PhysRevE.84.021303](https://doi.org/10.1103/PhysRevE.84.021303)

PACS number(s): 45.70.Vn, 02.60.Cb

**I. INTRODUCTION**

There is substantial literature dedicated to understanding inelastic particle collisions which covers applications ranging from pharmaceutical [1] powders and transporting fruit [2] to studying asteroids in the Saturnian ring system [3]. The current study is motivated by the practical aspects of simulating the processing of pharmaceutical powders on the scale of individual granules of active ingredient and excipients (e.g., binders). This requires an adequate physical description of interparticle contacts consistent with the available experimental data for both the material properties of granules themselves and the ways they interact with each other. For such a common pharmaceutical excipient as microcrystalline cellulose (MCC) it was shown recently that the average Young's modulus measured on a nanoscale by atomic force microscopy is similar to that measured macroscopically [4]. This is advantageous from the point of view of computer modeling as the elastic component of the intergranular contact forces can be readily parametrized. However, it is less clear how to describe the dissipative component both in terms of the model choice and its parameters.

The starting point for theoretical and computational studies of granular collisions is a contact model—a set of the constituent force laws describing contact forces and torques between the particles as they collide. There is always a restoring elastic force: either linear described by Hooke's law or nonlinear described by Hertz's law if the particles are considered to be elastic spheres. Energy dissipation is usually introduced into the model either via a velocity-dependent damping force [5,6] or via nonsymmetric loading-unloading force laws [7]. The fundamental problem here is that there

are a number of ways the energy is dissipated, but the overall effect has to be reproduced by an analytically or otherwise well-defined dissipative force. The physical mechanisms responsible for the energy dissipation include but are not limited to viscoelasticity, plastic deformation, bulk, and surface elastic waves. This is why the use of simplified contact models, such as a linear spring-dashpot (LSD) model or a Hookean spring-dashpot (HSD) model [8,9], can be justified as they provide a means of capturing the essential elastic and dissipative characteristics of the system. These two models, however, simply postulate the coefficient of restitution as a collision property which does not depend on the particles' impact velocity, elastic properties, or sizes. When using such simplified constitutive models, the model parameters have to be chosen empirically in order to match a given experimental system and there is no analytical route to predict how the variation of system parameters such as particle size or the material they are made of will affect the contact laws. The same is true for the variation of the experimental conditions such as, for example, the impact velocity in a two-particle collision. For this particular example, different models can be fitted to reproduce the experimentally observed energy dissipation at a given impact velocity, but as soon as collision velocity is changed, the models' predictions can be qualitatively different [5]. Therefore, it is important to have a better understanding of how a particular physical phenomenon, such as viscoelasticity, translates into appropriate constituent force laws and how these laws depend on the parameters of the collision.

For simplicity, we shall concentrate on head-on collisions of spherical granules without taking into account their rotational degrees of freedom. The energy dissipated in such a collision can be quantified by the normal restitution coefficient

$$\varepsilon = \left| \frac{v(\tau)}{v(0)} \right|, \quad (1)$$

\*jae1001@cam.ac.uk

where  $v(0)$  is the impact velocity and  $v(\tau)$  is the velocity at the end of the collision identified by collision time  $\tau$ . Note that the exact definition of “the end of the collision” will affect both  $\tau$  and  $\varepsilon$ .

The ball-drop experiment is a common way of measuring restitution coefficient  $\varepsilon$ . In such an experiment, a spherical object is dropped from a known height  $H$  and its rebound height  $h$  is measured. Then the restitution coefficient can be calculated as  $\varepsilon = \sqrt{h/H}$ . Experimental data indicates that the restitution coefficient decreases at higher collision velocities, though this decrease is often too small to differentiate between various contact models [10,11]. The dependence of the restitution coefficient on particle size is much less studied despite being crucial for the discrete element method (DEM) simulations of powders.

The main challenge is to decide on the restitution coefficient for microscopic (around 100  $\mu\text{m}$  in diameter) granules of powder from experimental data available for macroscopic spheres approximately 100 times larger in size. The two common choices are either (1) to assume that the restitution coefficient is independent of the particle size (and consequently the impact velocity) and use the HSD model or (2) use a viscoelastic or Hertz-Kuwabara-Kono (HKK) model in which the restitution coefficient decreases at higher impact velocities and then accept the size dependence predicted by this model. We investigate the second route and conduct a detailed analysis of how the input parameters of the HKK model affect both the restitution coefficient and collision time. Additionally, we demonstrate how nonspherical particles can be treated within the same formalism and how collision properties for the ball-drop experiment are related to those for a collision of two free viscoelastic spheres.

The remainder of this paper is structured as follows. We first describe the experimental and numerical methodology in Sec. II. Then, the justification for use of the HKK model, its details, and some exact analytical results are given in Sec. III. This is followed by the application of the HKK model to experimental data in Sec. IV. In Sec. V we demonstrate that if elastic, viscous, and cohesive forces are considered together in a single contact model, it predicts completely inelastic collisions (dissipative capture) even for very weak cohesive forces. Section VI summarizes our findings and suggests possible sources of the overestimated energy dissipation in microscopic particles.

## II. EXPERIMENTAL AND NUMERICAL METHODS

The restitution coefficient of nonspherical MCC tablets was measured experimentally using formula  $\varepsilon = \sqrt{h/H}$  by dropping them repeatedly on a large flat substrate, also made from compacted MCC, from a height  $H$  of up to 1 m and measuring their rebound height  $h$  by using a digital camera against a ruled scale [12]. The vacuum release mechanism was used to ensure that the tablets fell flat on their side and bounced off the substrate straight up as described in more details in Ref. [12].

The tablets were prepared by uniaxial compaction of MCC Avicel PH102 powder using two concave punches. For all tablets, the curvature radius was  $R = 5.26$  mm and the mass  $m = 500$  mg. The density of the tablets was  $\rho = 1.56$  g  $\text{cm}^{-3}$ ,

which is comparable to the bulk MCC density (i.e., the solid fraction close to 1 for both the tablet and the target). Note that using different grades of MCC powder with larger granules to produce the tablets did not significantly affect the solid fraction or restitution coefficient which was always within the 0.5 to 0.65 range. This supports the hypothesis that a densely compacted tablet can be treated as a continuous bulk material.

Numerical calculations were performed by integration of the Newtonian equation of motion using the leap-frog scheme. Initial position and velocity were used to start the calculation, while the force constants were determined by material parameters and particle sizes. For all MCC granule sizes we use bulk values of Young’s modulus  $E = 6$  GPa and the Poisson’s ratio  $\nu = 0.3$ , which is supported by recent AFM measurements [4].

## III. VISCOELASTIC CONTACT MODEL FOR PARTICLE COLLISION

### A. Model details

Consider a normal (i.e., head-on) collision of two spherical particles of radii  $r_1$  and  $r_2$ . We assume that the direction of the impact velocity  $v$  is colinear with the vector connecting the centers of the particles, as is the velocity after collision  $v'$ . Hence,  $\varepsilon = v'/v$ . If the particles are purely elastic and there is no energy dissipation ( $\varepsilon = 1$ ), the force between them is described by Hertz’s law:

$$F_{\text{el}}(\delta) = \frac{4E_{\text{eff}}\sqrt{r_{\text{eff}}}}{3}\delta^{\frac{3}{2}}, \quad (2)$$

where  $1/E_{\text{eff}} = (1 - \nu_1^2)/E_1 + (1 - \nu_2^2)/E_2$  is a function of the bulk material properties (Young’s moduli  $E_1$  and  $E_2$  and Poisson’s ratios  $\nu_1$  and  $\nu_2$ ),  $1/r_{\text{eff}} = 1/r_1 + 1/r_2$  is a function of the particles’ radii  $r_1$  and  $r_2$ , and the total deformation  $\delta$  is related to the separation between the particles’ centers  $r_1 + r_2 - \delta$ .

Note that force (2) does not change whether the target particle is fixed or not or if material properties of the particles are swapped around. These changes, however, will affect the collision properties via the effective mass  $m_{\text{eff}} = (1/m_1 + 1/m_2)^{-1}$  entering the equation of motion  $m_{\text{eff}}\ddot{\delta} = F_{\text{el}}(\delta)$ . Consider, for example, the maximum deformation  $\delta_{\text{max}}$  which can be determined by the conservation of energy in the zero momentum frame as the deformation at which the elastic energy  $E_{\text{el}} = \int_0^{\delta_{\text{max}}} F_{\text{el}}(\delta)d\delta$  is equal to the kinetic energy  $E_{\text{kin}} = m_{\text{eff}}v^2/2$ :

$$\delta_{\text{max}} = \left( \frac{15m_{\text{eff}}}{16E_{\text{eff}}\sqrt{r_{\text{eff}}}} \right)^{\frac{2}{5}} v^{\frac{4}{5}}. \quad (3)$$

Equation (3) predicts, for example, that the maximum deformation in a collision of two identical elastic spheres will increase by a factor of  $2^{\frac{2}{5}} \approx 1.32$  if one of them is fixed.

The collision time  $\tau$  will also depend on the details of the collision and for two identical elastic spheres is calculated analytically [13,14] as

$$\tau = 3.218 \left[ \frac{\pi\rho(1 - \nu^2)}{2E} \right]^{2/5} \frac{d}{v^{1/5}}. \quad (4)$$

TABLE I. Effective elastic and damping parameters  $E^*$  and  $D^*$  for four collision types involving a sphere and one of the listed targets made of the same material.

Target type	$m_{\text{eff}}$	$r_{\text{eff}}$	$E^*$	$D^*$
A. Fixed sphere	$m$	$d/4$	$2E$	$3D$
B. Plane	$m$	$d/2$	$2\sqrt{2}E$	$3\sqrt{2}D$
C. Free sphere	$m/2$	$d/4$	$4E$	$6D$
D. Free cylinder	$m/2$	$d/2$	$4\sqrt{2}E$	$6\sqrt{2}D$

Different loading-unloading protocols will affect the collision properties of two dissipative particles in a similar way. In particular, the restitution coefficient  $\varepsilon$  will depend on particle sizes (via  $r_{\text{eff}}$  and  $m_{\text{eff}}$ ), their mechanical properties (via  $E_{\text{eff}}$ ) and whether or not the target particle was fixed (via  $m_{\text{eff}}$ ), as will be shown later in Table I for the dissipative model described below.

The analytical expression for the dissipative force between viscoelastic spheres was first proposed by Kuwabara and Kono [15] and later derived by Brilliantov *et al.* [16] and Morgado and Oppenheim [17] using fundamentally different approaches. While a viscoelastic mechanism, that is, the energy dissipation being proportional to local deformation rate, is responsible for the energy loss in Ref. [16], the collision energy is adsorbed by harmonic lattice vibrations in Ref. [17]. Both models rely on the fact that the elastic force is described by Hertz's law and predict that the dissipative force can be written as

$$F_{\text{dis}}(\delta, \dot{\delta}) = D\sqrt{r_{\text{eff}}}\sqrt{\delta}\dot{\delta}, \quad (5)$$

where  $D$  is a material constant which has dimensions of viscosity and is either a function of viscosity material constants [15,16] or a number of microscopic material parameters [17]. In any case,  $D$  is a material property which sets the rate of the energy dissipation upon particle collision and does not depend on particle size, its Young's modulus (unlike parameter  $A = 0.5D/E_{\text{eff}}$  in Ref. [16]) or collision velocity.

Since, similar to the experimental observations, the HKK model predicts a lower coefficient of restitution at higher collision velocities and has a theoretical basis described above, it is widely used to simulate granular collisions. It also, for example, fits remarkably well the experimental data on collision of ice spheres at different velocities [16], despite the fact that the energy is dissipated as a result of fracture at the contact surface area of the ice particles. This arguably covers yet another mechanism for energy dissipation described by Eq. (5) and makes the choice of the HKK model more appealing.

From a practical point of view, it might be advantageous to follow an alternative route and predefine the restitution coefficient  $\varepsilon$  for a given collision. For that, the Hertzian elastic force (2) can be complemented by a fictitious dissipative force, which is known to be proportional to  $\sqrt[4]{\delta}$  [18] [rather than to  $\sqrt{\delta}$  in Eq. (5)] and is given by [9]

$$F_{\text{dis}}(\delta, \dot{\delta}) = \frac{-2 \ln \varepsilon}{\sqrt{\ln^2 \varepsilon + \pi^2}} \sqrt{\frac{5}{3}} \sqrt{E_{\text{eff}} m_{\text{eff}} \sqrt{r_{\text{eff}}} \delta \dot{\delta}}. \quad (6)$$

## B. Choice of reduced units for the HKK model

In the absence of gravity, the evolution of particles' deformation  $\delta$  is described by the sum of elastic and dissipative forces  $m_{\text{eff}}\ddot{\delta} = F_{\text{el}} + F_{\text{dis}}$ . By using Eqs. (2) and (5) and assuming that both particles are made of the same material we obtain

$$m_{\text{eff}}\ddot{\delta} = \frac{2E\sqrt{r_{\text{eff}}}\delta^{3/2}}{3(1-v^2)} + D\sqrt{r_{\text{eff}}}\sqrt{\delta}\dot{\delta}. \quad (7)$$

For the purposes of analysis and to obtain a numerical solution to Eq. (7), it is convenient to present it in dimensionless units. Since the duration of the collision depends on the impact velocity  $v$ , there is no characteristic time to describe such collisions. Therefore, the unit of time is often chosen to depend on  $v$  (see Refs. [15] and [14] for example). This definition, however, poses a problem when a large number of particles collide with each other at different velocities as, for example, in a powder flow or powder compaction simulations. As these simulations often include gravity, that is,  $g$  is the characteristic acceleration, there is a convenient way of defining the unit of time as  $\sqrt{d/g}$ , which is independent of the details of individual collisions. For the same reason, the maximum particle deformation  $\delta_{\text{max}}$  should not be used as the unit of length as in Ref. [15]. Instead, we use a particle diameter or, in the case of a polydisperse system, the smallest particle diameter as the unit length. If  $m$  is the mass of the particle with diameter  $d$ , then the forces are measured in units of  $mg$ , the unit of energy is  $mgd$ , the unit of pressure is  $mg/d^2$ , and the unit of velocity is  $\sqrt{gd}$ .

For a free collision of two identical spheres, that is, when  $r_1 = r_2 = d/2$ ,  $r_{\text{eff}} = d/4$ , and  $m_{\text{eff}} = m/2 = \frac{\pi}{12}d^3\rho$ , Eq. (7) reads

$$\ddot{\delta}^* = \frac{4E\delta^{*3/2}}{g\rho\pi d(1-v^2)} + \frac{6D\sqrt{\delta^*}\dot{\delta}^*}{\sqrt{g\rho\pi}d^{3/2}}, \quad (8)$$

where the reduced units are marked by an asterisk and  $\rho$  is the material density.

To include other collision types summarized in Table I, Eq. (8) can be generalized to

$$\ddot{\delta}^* = \frac{E^*\delta^{*3/2}}{g\rho\pi d(1-v^2)} + \frac{D^*\sqrt{\delta^*}\dot{\delta}^*}{\sqrt{g\rho}d^{3/2}}, \quad (9)$$

where parameters  $E^*$  and  $D^*$  are, respectively, proportional to the Young's modulus  $E$  and damping parameter  $D$ . The data in Table I are obtained assuming that the masses of a fixed particle or a plane are infinite. For collision type D we assume that the sphere collides with the flat side of the cylinder (i.e.,  $r_2 = \infty$ ) and both bodies have the same mass (i.e.,  $m_1 = m_2$ ) similar to the experimental setup in Ref. [19].

## C. The end of the collision

It was previously demonstrated that the end of the collision must be identified as the moment when the total force becomes zero, that is,  $\ddot{\delta} = 0$ , not when the deformation turns to zero, that is,  $\delta = 0$  [14]. Here we briefly explain the importance of these findings and demonstrate how they affect collision properties.

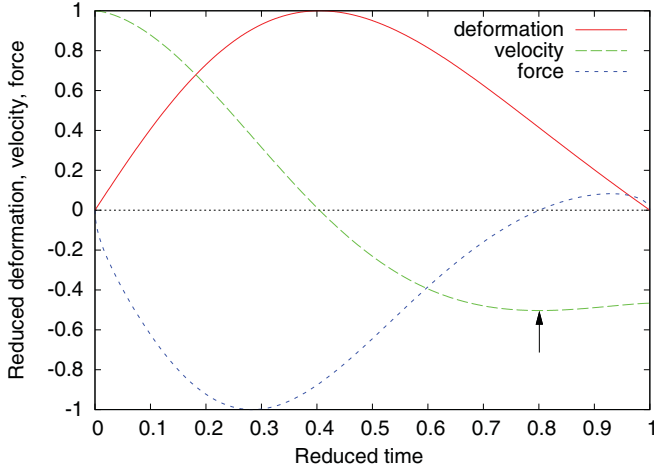


FIG. 1. (Color online) The deformation, the rate of the deformation, and viscoelastic force during a collision of two viscoelastic particles characterized by a restitution coefficient of 0.5. All quantities are normalized by their maximum values.

Figure 1 shows the numerical solution for the deformation, its rate, and the viscoelastic force normalized by their maximum values for a sample collision in which around three-quarters of the kinetic energy is dissipated (i.e.,  $\varepsilon = \sqrt{E_{\text{after}}/E_{\text{before}}} = 0.5$ ). While for an elastic collision, the time it takes to reach the maximum deformation is exactly half of the collision time, in the case of an inelastic collision, the displacement curve is no longer symmetrical. After the velocity of the deformation passes through zero and the particles start moving away from each other, the velocity passes through a minimum as indicated by the arrow in Fig. 1. At this point the magnitude of the damping force opposing the high particle velocity becomes greater than that of the elastic force. This is the point which corresponds to the end of the collision. When the total force becomes positive (around  $t^* = 0.80$  in Fig. 1) the colliding particles lose contact while still being deformed. This event has to be taken into account by replacing the unphysical attractive force with a value of zero despite some deformation still being present. Otherwise, the particle will experience attraction which has no physical basis in the HKK model and the final particle velocity will be underestimated, resulting in a lower value of the restitution coefficient. In Fig. 2 we demonstrate this effect for a collision of two viscoelastic particles parametrized using material properties of microcrystalline cellulose (MCC). The asymptotic behavior of the restitution coefficient changes depending on the criterion used to identify the end of the collision. The values for the asymptotic gradients shown in Fig. 2 were obtained from numerical calculations with various time steps at extreme damping and collision velocities and were verified with accuracy of one part per million (cf. value of  $-0.331$  instead of  $-1/3$  in Ref. [14]).

When the incorrect  $\delta = 0$  criterion is used to determine the end of the collision for the dissipative particles, the collision time becomes greatly overestimated at large impact velocities. Figure 3 shows the collision time for the same viscoelastic spheres as above. The dotted line in Fig. 3 is the theoretical prediction of the collision time for purely elastic spheres, that is, the time given by Eq. (4).

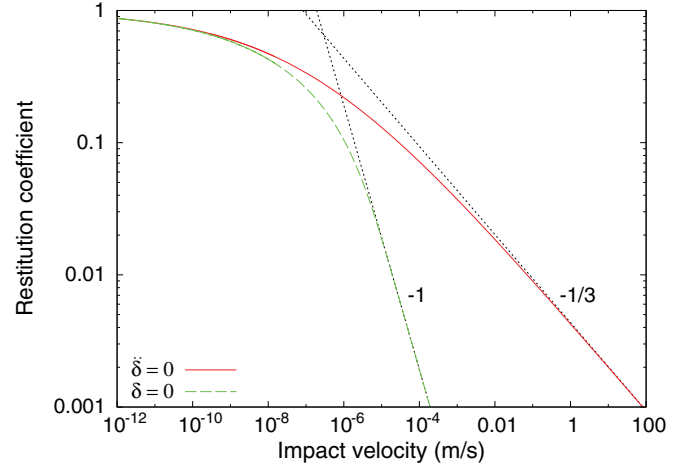


FIG. 2. (Color online) Calculated restitution coefficient of two identical  $100 \mu\text{m}$  spheres with MCC material properties as a function of the impact velocity calculated according to two different criteria to define the end of the collision: correct  $\tilde{\delta} = 0$  (solid red line) and incorrect  $\delta = 0$  (dashed green line). The dotted lines are asymptotes calculated numerically with their gradients shown.

#### D. Scaling properties of the HKK model

It has been previously shown that for the HKK model both the coefficient of restitution and collision time can be approximated by power series of  $v^{1/5}$  [20,21]. A different series expansion was used in Ref. [14] to show that  $\varepsilon$  is a unique function of the following combination of parameters (in our notation):  $DE^{-3/5}v^{1/5}$ . The collision time  $\tau$  can also be considered as a function of the combination above if the unit of time is rescaled proportionally to  $DE$ . For the choice of dimensionless variables we use in this paper, it can be shown analytically (similarly to Ref. [14]) and verified numerically

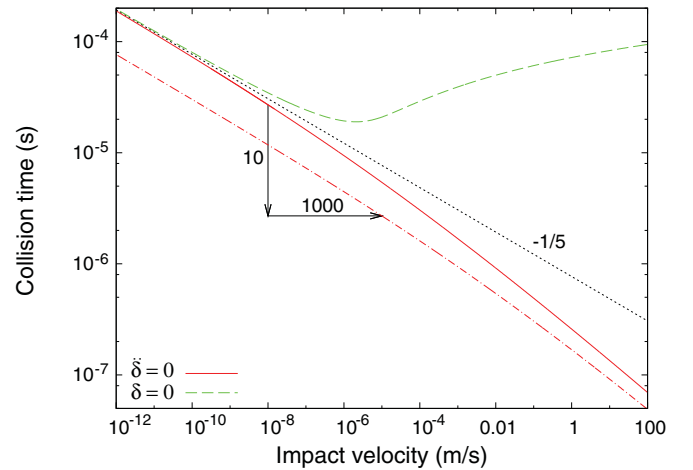


FIG. 3. (Color online) Collision time of two identical  $100 \mu\text{m}$  spheres with MCC material properties as a function of the impact velocity calculated according to two different criteria to define the end of the collision: correct  $\tilde{\delta} = 0$  (solid red line) and incorrect  $\delta = 0$  (dashed green line). The black dotted line is the asymptote calculated using Eq. (4) with the gradient of  $-1/5$  as indicated. The red dot-dashed line is obtained for a material with Young's modulus 10 times greater than that of the MCC by shifting the solid line according to the rules given in Table II.

that both  $\varepsilon(v)$  and  $\tau(v)$  are unique functions of  $d\rho^{2/5}$ . As shown above, these scaling properties can be extended to include the collision type via effective elastic and damping parameters  $E^*$  and  $D^*$ . In general, two collisions which have the same values of  $D^*E^{*-3/5}v^{1/5}d^{-1}\rho^{-2/5}$  will have identical restitution coefficients. In fact,  $1 - \varepsilon$  is proportional to this combination of parameters [15,22] for nearly elastic collisions (note the typographical error in Eq. (11) of Ref. [22] where  $\rho^{-2/5}/E^{3/5}$  is rendered as  $\rho^{2/5}/E^{-3/5}$ ).

From a practical point of view, this means that any change in the parameters present in Eq. (9) does not change the shape of the curves (shown in Figs. 2 and 3 and calculated as a series expansion in Ref. [14]) but only shifts their positions. Note that this statement is true for using either the  $\delta = 0$  or  $\delta = 0$  criterion to define the end of the collision. In Table II we summarize what shifts the  $\varepsilon(v)$  and  $\tau(v)$  curves experience if one of the model parameters is multiplied by a factor  $\alpha$ . For example, to predict a collision time for two 100  $\mu\text{m}$  spheres made of a material 10 times stiffer than, but otherwise identical to, MCC, according to Table II, one has to shift the solid red curve shown in Fig. 3 down by 10 and right by 1000, as shown by the dot-dashed red line. Note that the transformations in Table II are true for both elastic and viscoelastic particles. As expected, for purely elastic particles the transformations for  $\tau$  are consistent with the predictions of Eq. (4).

Since  $\varepsilon(v)$  decreases monotonically with  $v$ , the damping  $D^*$  is the only parameter whose increase will reduce  $\varepsilon$  when measured at the same impact velocity. At the same time, larger values for  $E^*$ ,  $d$ , and  $\rho$  will result in higher restitution coefficients, that is, stiffer, larger, and heavier particles dissipate less energy.

Using the transformations given in Tables I and II, it is straightforward to relate the restitution coefficient measured in a ball-drop experiment (collision type B in Table I) to that expected for a collision of free spheres (collision type C). Both elastic and dissipative terms for the sphere-sphere collision are  $\sqrt{2}$  times greater than those for the sphere-plane collision. According to Table II, the simultaneous increase of  $E$  and  $D$  by  $\alpha = \sqrt{2}$  is equivalent to applying the left shift by  $\alpha^{5-3} = 2$  to both  $\varepsilon(v)$  and  $\tau(v)$  curves. This means that the impact velocity in the ball-drop experiment has to be halved to reproduce the restitution coefficient seen in a sphere-sphere collision. Due to the monotonic behavior of  $\varepsilon(v)$ , the restitution coefficient for a sphere-plane collision will always be higher than that for two free spheres at a given impact velocity (see Fig. 4 for example).

The transformation between any two collision types in Table I can be obtained in a similar way. To summarize, with

TABLE II. This table shows how the restitution coefficient  $\varepsilon$  and collision time  $\tau$  curves, shown correspondingly in Figs. 2 and 3, will shift if a given parameter  $X$  in Eq. (9) is replaced by  $\alpha X$ .

$X$	$\varepsilon$	$\tau$
Elasticity, $E^*$	right by $\alpha^3$	down by $\alpha$ and right by $\alpha^3$
Damping, $D^*$	left by $\alpha^5$	up by $\alpha$ and left by $\alpha^5$
Diameter, $d$	right by $\alpha^5$	right by $\alpha^5$
Density, $\rho$	right by $\alpha^2$	right by $\alpha^2$

all other factors being equal, a free sphere-cylinder collision (D) dissipates most energy, followed by a free sphere-sphere collision (C), then a sphere-plane collision (B), whereas a sphere-sphere collision with the target sphere fixed dissipates least energy.

#### IV. APPLICATION OF THE VISCOELASTIC MODEL TO EXPERIMENTAL DATA

##### A. Finding damping parameter $D$ from experiment

In this section the transformations shown in Tables I and II are used to find the material parameter  $D$  from data collected in a ball-drop experiment using a 1 cm nonspherical tablet with axial symmetry and two convex faces.

Since the tablets used in our experiment were nonspherical (as illustrated in Fig. 4), a sphere with the same curvature and density will be heavier and hence have a higher restitution coefficient. The particle mass enters Eq. (7) only via material density  $\rho$ , which can be adjusted so that the nonspherical tablet is treated as a lighter sphere. Taking the mass ratio between the 500 mg MCC tablet and an MCC sphere with the same curvature of mass  $m = 4/3\pi R^3\rho = 951$  mg, we can predict that the  $\varepsilon(v)$  curve for this sphere will be shifted to the right by  $(951/500)^2 \approx 1.9^2 \approx 3.62$ . Figure 4 shows the  $\varepsilon(v)$  curve (blue solid line) that was fitted to the experimental data using the method of least squares. Though the theory provides an adequate fit to the experimental data with  $D = 12000 \text{ kg m}^{-1}\text{s}^{-1}$ , the converse statement that the use of the HKK model is supported by the experiment or that MCC is a viscoelastic material is not true. Indeed, some plastic deformation is expected especially at high collision velocities [12], which might be responsible for a slightly steeper gradient of the experimental data than that predicted by theory.

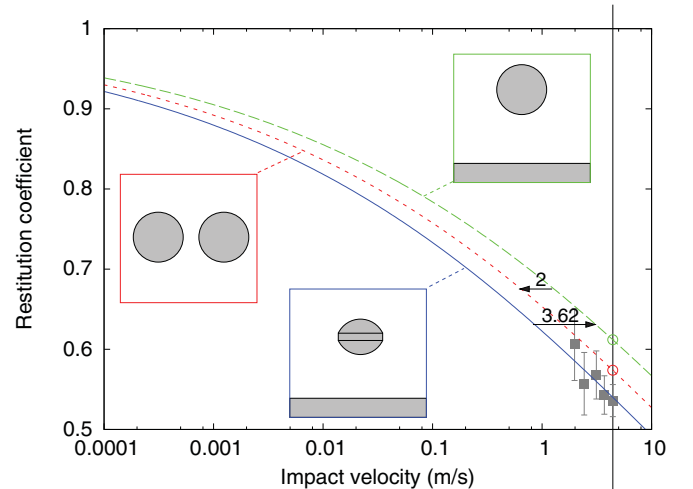


FIG. 4. (Color online) Restitution coefficient measured for an axisymmetric biconvex MCC tablet (gray squares with the error bars indicating standard deviation) and fitted using HKK theory (blue solid line). The  $\varepsilon(v)$  curves for a sphere-plane and a free collision of two spheres with the same curvature radius (shown as the green and red dashed lines, respectively) were obtained by applying the indicated shifts along the  $x$  axis as described in the text. The vertical line indicates the collision velocity  $v = \sqrt{2gH} = 4.43 \text{ m s}^{-1}$  corresponding to the drop height of  $H = 1 \text{ m}$ .

Assuming that the HKK model is applicable to describe our model material, the  $\varepsilon(v)$  curve for a free collision of two spherical granules can be obtained by shifting the sphere-plane curve to the left by a factor of 2 as discussed above in Sec. III. Figure 4 shows all three collisions and the corresponding  $\varepsilon(v)$  curves. At  $v = 4.43 \text{ m s}^{-1}$ , the restitution coefficient for the sphere-plane collision is  $\varepsilon = 0.612$ , and  $\varepsilon = 0.574$  for the free sphere-sphere collision, both marked by the open circles in Fig. 4.

For a free sphere-cylinder collision (type D in Table I, not shown in Fig. 4), the viscoelastic model predicts a restitution coefficient approximately 6% lower than that for two spheres (type C). This contrasts with results for collisions with plastic deformation which predict  $\varepsilon$  for collision D to be 19% higher than for collision C [19].

### B. Dependence of restitution coefficient on particle size

Assuming that the damping parameter  $D$  obtained from the experimental data in the previous section is a material property which is not affected by the particle size, we now calculate the restitution coefficient for smaller but still macroscopic spheres bouncing off a plane, that is, the ball-drop experiment. To make the results comparable, the drop height  $H$  is fixed at  $H = 100d$  and three diameters  $d = 1 \text{ cm}$ ,  $d = 1 \text{ mm}$ , and  $d = 0.1 \text{ mm}$  are considered.

We solve Eq. (7) numerically with [Fig. 5(a)] and without [Fig. 5(b)] addition of the gravitational force to this equation. When a gravitational force is included in Eq. (7), it introduces a cutoff impact velocity below which the incident particle does not separate from the plane after the collision but remains in contact with it. When this happens, the particle continues to oscillate around the equilibrium deformation  $\delta_0$  while gradually dissipating energy at the same time. If the impact velocity is relatively high, the incident particle will bounce a finite number of times [as shown by the circles in Fig. 5(a)] until it reaches the regime described above. It is evident from Fig. 5(a) that smaller particles reach equilibrium much faster than larger particles. Indeed, the smallest particle

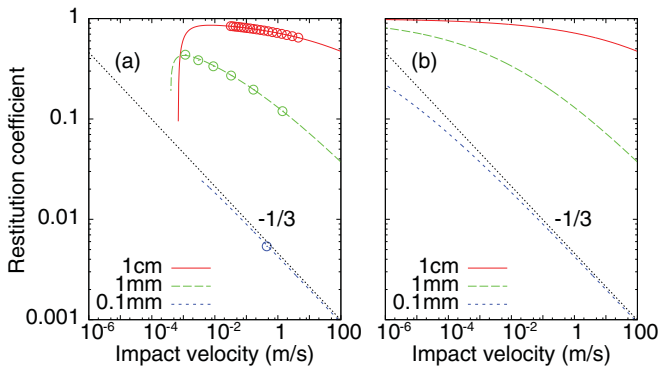


FIG. 5. (Color online) Calculated restitution coefficient for a viscoelastic sphere with material parameters of MCC bouncing off a plane (a) with and (b) without the effect of the gravitational field. The circles correspond to consecutive rebounds of a sphere dropped from a height of  $100d$  in a computer simulation with gravity. All data were obtained by solving Eq. (7) numerically for the different impact velocities  $v$ .

TABLE III. Relationship between the coefficient of restitution in a ball-drop experiment with  $H = 100d$  for particles with diameter  $d$  (as input values for different materials) and particles with diameter  $0.01d$  (as predicted by the HKK model).

$\varepsilon$ for diameter $d$	0.5	0.6	0.7	0.8	0.9
$\varepsilon$ for diameter $0.01d$	0.0002	0.0041	0.0079	0.0174	0.0552

experiences only one rebound with  $\varepsilon = 0.0045$ , while the number of rebounds is greater than one for larger particles. This reduction of the coefficient of restitution is a generic feature of the HKK contact model and affects any material with viscoelastic behavior as demonstrated in Table III.

Figure 5(b) shows the restitution coefficient for the collisions in the absence of the gravitational field. Note that all three curves in Fig. 5(b) have the same shape and are shifted in respect to each other by five orders of magnitude along the  $x$  axis, as predicted by transformations in Table II for a tenfold change in the particle diameter. The curves in Fig. 5(a) have different shapes because the addition of gravity (or any attractive interactions for that matter) breaks the scaling properties of the HKK model. Both parts of Fig. 5 show the same straight dotted line corresponding to the asymptote with a gradient of  $-1/3$  also shown in Fig. 2. The reduction of the restitution coefficient due to gravity seen in Fig. 5(a) at low impact velocities has also been observed experimentally [10]. Note that in our analysis and in Ref. [10], any correlations between the forces are neglected. This is not strictly true because gravity will increase the contact area which in turn is expected to increase the dissipative force.

### V. EFFECT OF COHESIVE FORCES

To ensure that a tablet remains intact after it has been compacted, the cohesive energy of pharmaceutical powders is typically high [23]. The last section of this paper is therefore concerned with energy dissipation in the presence of cohesive forces. First, we discuss ways of combining the elastic, dissipative, and cohesive force in a single model, then we consider collisions of cohesive particles using parameters of MCC as an example.

When no cohesion is present, the damping force due to material viscosity is defined by Eq. (5), that is, the HKK model. In the HKK model the radius of the contact spot  $a$  is exactly  $a = \sqrt{r_{\text{eff}}\delta}$ , and the dissipative force described by Eq. (5) can be written as

$$F_{\text{dis}} = Da\dot{\delta}. \quad (10)$$

In the presence of cohesion, the size of the contact spot is greater at the same deformation  $\delta$ . The magnitude of the dissipative force is also expected to increase since more material is deformed at approximately the same speed during the particle collision when compared to the cohesion-free case. The relationship between  $\delta$  and  $a$  for the cohesive nondissipative particles described by the Johnson-Kendall-Roberts (JKR) model [24] is

$$\delta(a) = \frac{a^2}{r_{\text{eff}}} - \sqrt{\frac{2\pi\gamma a}{E_{\text{eff}}}}, \quad (11)$$

where  $\gamma$  is the surface energy. The expression for the total force due to the elasticity and cohesion reads

$$F_{\text{JKR}}(a) = \frac{4E_{\text{eff}}a^3}{3r_{\text{eff}}} - \sqrt{8\pi\gamma E_{\text{eff}}a^3}. \quad (12)$$

From  $F_{\text{JKR}}(a) = 0$ , we can find the equilibrium contact radius

$$a_0 = \left( \frac{9\pi\gamma r_{\text{eff}}^2}{2E_{\text{eff}}} \right). \quad (13)$$

Equations (11) and (12) expressed in terms of  $a_0$  become

$$\delta(a) = \frac{a^2}{r_{\text{eff}}} \left( 1 - \frac{2}{3} \sqrt{\frac{a_0^3}{a^3}} l \right) \quad (14)$$

and

$$F_{\text{JKR}}(a) = \frac{4E_{\text{eff}}a^3}{3r_{\text{eff}}} \left( 1 - \sqrt{\frac{a_0^3}{a^3}} \right). \quad (15)$$

The analysis of Eqs. (14) and (15) shows that as the two particles move away from each other, the contact area decreases monotonically and the net force remains attractive for all  $a < a_0$ . Condition  $\delta(a) = 0$  is reached when contact radius is  $a \approx 0.76a_0$ . At  $\delta(a) < 0$ , the particles remain in contact as the maximum force  $F_{\text{pull-off}} = -3\pi\gamma r_{\text{eff}}$  is reached when  $a \approx 0.63a_0$ . After this point, the attractive force  $F_{\text{JKR}}(a)$  starts to decrease until the particles suddenly lose contact at  $a \approx 0.30a_0$  when  $F = 5/9F_{\text{pull-off}}$  [25].

An *ad hoc* way of incorporating energy dissipation in the JKR model would be simply to use Eq. (5) with the actual displacement  $\delta$  (or rather  $\sqrt{\delta}$ ) or by using Eq. (10) with the actual contact spot radius  $a$  found from Eq. (11). The first approach, used in Ref. [3], is limited to positive values of  $\delta$  and therefore cannot make any predictions for negative  $\delta$ . The second approach is qualitatively correct but was shown to overestimate the amount of energy dissipation [26]. In Ref. [26] the energy dissipation was shown to be simply proportional to the time derivative of the contact force (12), that is,  $F_{\text{dis}}(a) = A\dot{a} \frac{\partial F_{\text{JKR}}(a)}{\partial a}$ , where  $A = 0.5D/E_{\text{eff}}$  in our notation. By substituting  $\dot{a} = \dot{\delta} \frac{\partial a}{\partial \delta}$  into this equation we obtain

$$F_{\text{dis}}(a) = Da \left( 1 - \frac{2}{6\zeta - 1} \right) \dot{\delta}, \quad (16)$$

where  $\zeta = \sqrt{a^3/a_0^3}$  is a dimensionless parameter reciprocal to that seen in Eqs. (14) and (15). Note that at equilibrium, that is,  $a = a_0$  and  $\zeta = 1$ , Eq. (16) predicts energy dissipation 40% lower than that predicted when the term dependent on  $\zeta$  is neglected. At higher deformations, the effect of this term is lower. Since the force in Eq. (16) is proportional to  $\dot{a}$ , it diverges when the particles lose contact at  $a \approx 0.30a_0$ , where  $\zeta = 1/6$ . Moreover, when  $F_{\text{pull-off}}$  is reached at  $\zeta = 1/2$ ,  $F_{\text{dis}}(a)$  becomes zero and it remains attractive till it diverges at smaller  $a$ . To avoid this unphysical behavior, we choose to use a simpler model described by Eq. (10) which is more computationally efficient and numerically stable.

Similarly to the effect of gravity, the presence of cohesive forces means that it is possible for the particles to remain in contact (i.e., “stick together”) if the impact velocity  $v$  is sufficiently low. As a result, a typical  $\varepsilon(v)$  profile for a

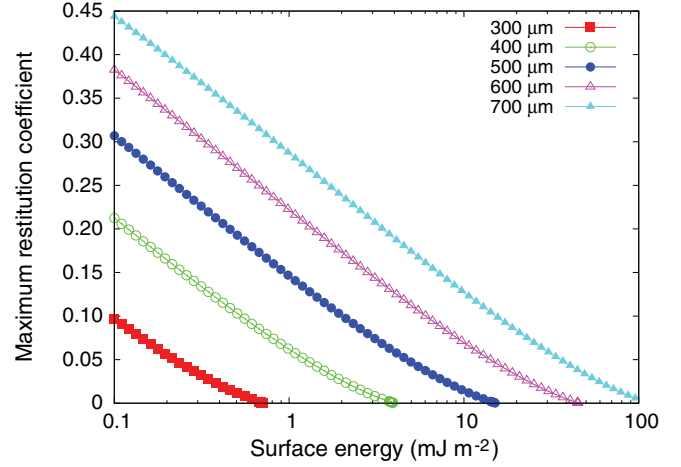


FIG. 6. (Color online) Maximum restitution coefficient predicted for spherical MCC granules as a function of their surface energy for different particle diameters, as indicated.

collision of viscoelastic cohesive particles looks similar to the curves shown in Fig. 5(a)—there is a well-defined maximum at moderate values of  $v$ . Figure 6 shows how this maximum value of the restitution coefficient changes with the surface energy  $\gamma$  for several particle diameters in the submillimeter range. For the smallest particles shown here, that is, 300  $\mu\text{m}$  in diameter, the particles are predicted to remain in contact if their surface energy is larger than  $\gamma \approx 0.71 \text{ mJ m}^{-2}$  no matter how high their relative velocity. This effect of dissipative capture is possible due to the combination of the viscous and cohesive forces—the viscous force reduces the kinetic energy so much that even weak cohesion is able to keep the particles together. As was shown in Sec. IV, smaller particles dissipate energy more effectively and therefore stick together at lower surface energies. The experimental value of MCC surface energy is around  $70 \text{ mJ m}^{-2}$  [23]. This means that particles smaller than about 650  $\mu\text{m}$  will be held together by cohesive forces once they are brought in contact.

At first glance this finding appears to contradict the experimental observation that much smaller MCC particles form dry powders without sticking together. However, what must be taken into account is that (1) the particles with coarse, rough surfaces would have a smaller effective surface energy, (2) the “stickiness” of the powder is assessed experimentally by applying macroscopic stresses much greater than those present in a binary collision, and (3) the presence of dissipation mechanisms other than viscoelastic will affect how the restitution coefficient changes with particle size and not necessarily result in the large reduction predicted by the HKK model alone.

The predicted ultralow restitution coefficients for submillimeter granules raises a question whether finding the damping parameter  $D$  is needed at all. For weakly cohesive powders, it is reasonable to assume that all collisions are purely inelastic and describe them, for example, by a critically damped Hertzian spring with  $\varepsilon = 0$  in Eq. (6).

## VI. CONCLUSIONS

In this paper we have shown that the restitution coefficient of viscoelastic particles described by the Hertz-Kuwabara-Kono (HKK) model is a unique function of the following

combination of parameters  $D^* E^{*-3/5} v^{1/5} d^{-1} \rho^{-2/5}$ . The effect of varying elasticity  $E$  and damping parameter  $D$ , the particle's diameter  $d$  and density  $\rho$  can be reduced to an appropriate rescaling of the impact velocity  $v$  (the only parameter in the expression above which is not the property of the colliding bodies) to predict the new restitution coefficient. Collision details (e.g., fixed or free target) and geometry (e.g., collision with a plane or a sphere) can also be taken into account by adjusting  $E$  and  $D$  as signified by an asterisk. Similar scaling can be applied to the collision time, except the time scale must also be changed as shown in Table I.

We used the scaling properties of the HKK model to demonstrate how the restitution coefficient measured experimentally for nonspherical tablets in a ball-drop experiment can be related to that for freely moving spherical particles. The material constant  $D$  responsible for viscous damping was obtained from a fit to the experimental data. For MCC tablets, the parameter  $A = D(1 - v^2)/E = 1.8 \times 10^{-6}$  s was found to be approximately 55 times weaker than that reported in the literature for ice particles [16,26]. Using this value, we simulated the collision of viscoelastic particles of different diameters with a plane. Our calculations summarized in Table III clearly indicate that collisions involved smaller particles are characterized by much lower restitution coefficients than those involved larger particles. Combined with the fact

that smaller particles have smaller masses, the dissipated energy is predicted to increase their temperature significantly during such powder processing as compaction [27]. This can be crucial for the tableting of pharmaceutical powders, where the increase in temperature can affect the properties of the drug [28,29].

We also discussed the application of viscous damping alongside the JKR model. A simple model in which the dissipative force is proportional to the contact radius was chosen due to its simplicity and numerical stability. This model becomes identical to the HKK model in the limit of the weak cohesive interactions. The quantitative analysis of this model predicted dissipative capture for particles in the submillimeter size range even if relatively weak cohesion was present. While this suggests that most granular collisions in a powder flow are completely inelastic, this is partially due to the overestimated energy dissipation when the HKK model is used alone to account for the energy loss. Experimental data for collision of macroscopic nylon spheres of different diameters also confirms that the HKK model overestimates the energy dissipation for smaller spheres [22], and therefore should not be used across two orders of magnitude of particle sizes.

#### ACKNOWLEDGMENT

We would like to thank Pfizer for funding this project, and Dr. Rahul Bharadwaj for help in obtaining experimental data.

- 
- [1] W. R. Ketterhagen, M. T. A. Ende, and B. C. Hancock, *J. Pharm. Sci.* **98**, 442 (2009).
  - [2] M. V. Zeebroeck, E. Tijssens, E. Dintwa, J. Kafashan, J. Loodts, J. D. Baerdemaeker, and H. Ramon, *Postharvest Biol. Technol.* **41**, 92 (2006).
  - [3] N. Albers and F. Spahn, *Icarus* **181**, 292 (2006).
  - [4] P. Laity, A. Cassidy, J. Skepper, B. Jones, and R. Cameron, *Eur. J. Pharm. Biopharm.* **74**, 377 (2009).
  - [5] J. Schäfer, S. Dippel, and D. Wolf, *J. Phys. I (France)* **6**, 5 (1996).
  - [6] S. Antonyuk, S. Heinrich, J. Tomas, N. G. Deen, M. S. van Buijtenen, and J. A. M. Kuipers, *Granular Matter* **12**, 15 (2010).
  - [7] O. R. Walton and R. L. Braun, *J. Rheol.* **30**, 949 (1986).
  - [8] K. F. Malone and B. H. Xu, *Particuology* **6**, 521 (2008).
  - [9] D. Antypov and J. A. Elliott, *Europhys. Lett.* **94**, 50004 (2011).
  - [10] E. Falcon, C. Laroche, S. Fauve, and C. Coste, *Eur. Phys. J. B* **3**, 45 (1998).
  - [11] A. Stevens and C. Hrenya, *Powder Technol.* **154**, 99 (2005).
  - [12] R. Bharadwaj, C. Smith, and B. C. Hancock, *Int. J. Pharm.* **402**, 50 (2010).
  - [13] L. D. Landau and E. M. Lifshitz, *Theory of Elasticity* (Elsevier, New York, 1986).
  - [14] T. Schwager and T. Pöschel, *Phys. Rev. E* **78**, 051304 (2008).
  - [15] G. Kuwabara and K. Kono, *Jpn. J. Appl. Phys.* **26**, 1230 (1987).
  - [16] N. V. Brilliantov, F. Spahn, J.-M. Hertzsch, and T. Pöschel, *Phys. Rev. E* **53**, 5382 (1996).
  - [17] W. A. M. Morgado and I. Oppenheim, *Phys. Rev. E* **55**, 1940 (1997).
  - [18] Y. Tsuji, T. Tanaka, and T. Ishida, *Powder Technol.* **71**, 239 (1992).
  - [19] G. Weir and S. Tallon, *Chem. Eng. Sci.* **60**, 3637 (2005).
  - [20] T. Schwager and T. Pöschel, *Phys. Rev. E* **57**, 650 (1998).
  - [21] R. Ramirez, T. Pöschel, N. V. Brilliantov, and T. Schwager, *Phys. Rev. E* **60**, 4465 (1999).
  - [22] L. Labous, A. D. Rosato, and R. N. Dave, *Phys. Rev. E* **56**, 5717 (1997).
  - [23] Z. Tüske, G. Regdon, I. Erős, S. Srčić, and K. Pintye-Hódi, *Powder Technol.* **155**, 139 (2005).
  - [24] K. L. Johnson, K. Kendall, and A. D. Roberts, *Proc. R. Soc. London Ser. A* **324**, 301 (1971).
  - [25] K. Johnson, *Contact Mechanics* (Cambridge University Press, Cambridge, 1987).
  - [26] N. V. Brilliantov, N. Albers, F. Spahn, and T. Pöschel, *Phys. Rev. E* **76**, 051302 (2007).
  - [27] A. Zavalianos, S. Galen, J. Cunningham, and D. Winstead, *J. Pharm. Sci.* **97**, 3291 (2008).
  - [28] L. H. Han, P. R. Laity, R. E. Cameron, and J. A. Elliott, *J. Mater. Sci.* **46**, 5977 (2011).
  - [29] G. Zhang, D. Law, E. Schmitt, and Q. Y., *Adv. Drug. Deliv. Rev.* **56**, 371 (2004).